*International Journal of Research and Review*
*[Indexed, Peer-Reviewed Journal]*
*Volume 13; Issue: 6; June 2026*
*Website: www.ijrrjournal.com*
*Research Paper* *E-ISSN: 2349-9788; P-ISSN: 2454-2237*

# Active Filter Solution for Three-Phase System Four Wires under Unbalanced and Harmonics Condition

**Tazkiya Muthmainnah Sukmawati[1], Susatyo Handoko[1], Mochammad Facta[1], Trias Andromeda[1], Karnoto[1]**

[1]Department of Electrical Engineering, Diponegoro University, Semarang, Indonesia.

Corresponding Author: Tazkiya Muthmainnah Sukmawati, Karnoto

**DOI: https://doi.org/10.52403/ijrr.20260619**

## ABSTRACT

This paper offers an assessment of the performance of an active filter (AF) with three phases and four wires. The suggested three-phase four-wire AF utilizes a split-capacitor configuration. It employs instantaneous active and reactive power theory to create the reference current as well as an adaptive hysteresis current controller to produce the switching signal. The assessment centers on the AF's capability to rectify existing current harmonic distortion and current imbalance in a three-phase four-wire configuration. All assessments were performed in line with IEEE 519-2022 and IEEE 1159-2019, which deal with current harmonic distortion and current imbalance in electrical systems. According to IEEE 519-2022, current harmonic distortion is analyzed using total demand distortion, with thresholds set by the calculated $I_{SC}/I_L$ ratio, a method not often addressed in other studies. Another important contribution of this paper is the application of IEEE 1159 as the standard for current imbalance, as limited research has assessed compensation performance for current imbalance with this standard. The assessment outcomes indicate that the AF introduced in this paper performs exceptionally in concurrently addressing current imbalance and current harmonics within a three-phase system with four wires.

***Keywords:*** *Active filter, Three-phase four-wire systems, Current harmonic distortion, Current imbalance, IEEE 519, IEEE 1159*

## INTRODUCTION

The ongoing rise in electricity usage over time has resulted in a higher number of loads, encompassing non-linear loads. As the term suggests, non-linear loads consume current with a waveform that strays from an ideal waveform, often called a distorted waveform. Contemporary power electronic devices, powered by switch-mode power supplies (SMPS), represent a major class of non-linear loads in electrical systems [1]. Along with generating current distortion, many of these devices operate as single-phase loads. In a three-phase system with four wires, the unequal allocation of single-phase loads across the three phases results in negative-sequence and zero-sequence components, leading to current imbalance [2]. The occurrence of current distortion and current imbalance in power systems elevates neutral current, potentially resulting in equipment damage, shorter lifespan, and diminished efficiency [3].

Mitigation measures are necessary to minimize the negative impacts of current harmonic distortion and current imbalance. A commonly utilized method is the active filter (AF). AF are recognized for their capability to compensate several harmonic orders and dynamically balance load currents across

different system characteristics [4]. AF are typically advised for implementation in a three-phase system with four wires due to their ability to act as both compensators for current harmonic distortion and current imbalance at the same time [5].

The effectiveness of an AF with three phases and four wires is usually evaluated based on its ability to reduce current harmonic distortion and current imbalance to meet standard limit values. The most commonly used international standard regarding current harmonic distortion is IEEE 519. IEEE 519 defines current harmonic distortion thresholds in terms of total demand distortion (TDD) percentages with mappings based on ratio of short-circuit current to load current ($I_{SC}/I_L$) [6]. Meanwhile, IEEE 1159 is one of the standards frequently used as a reference for monitoring current imbalance in electrical systems. IEEE 1159 explicitly classifies current imbalance as a long-duration power quality disturbance under steady-state conditions that must be monitored to ensure it remains within the specified typical range [7].

Although IEEE 519 is widely used in previous research, current harmonic distortion values are primarily evaluated based on the total current harmonic distortion ($THD_I$) percentage. Many papers mention that the $THD_I$ limit based on IEEE 519 is 5%, but there is no explanation regarding the $I_{SC}/I_L$ ratio used to determine this thresholds [8]–[16]. Some papers also indicate that AF is capable of reducing current imbalance in three-phase four-wire systems, however they do not specify the current imbalance standard used as a reference [11], [16], [17].

This paper examines current harmonic distortion values based on TDD percentages by refereeing to standard of IEEE 519-2022 and IEEE 1159-2019. This paper determines the TDD threshold value based on the calculated $I_{SC}/I_L$ ratio. Additionally, another contribution of this paper is the evaluation of current imbalance compensation performance in accordance with the IEEE 1159 standard. The application of this standard presents a novel approach to evaluating the performance of an AF with three phases and four wires, a topic that has received limited attention in previous papers.

## MATERIALS & METHODS

### System and Filter Configuration

In this paper, the test system used is a three-phase electrical system with four wires. The system is supplied by an ideal three-phase source with the distribution network modeled as source-side network impedance ($Z_S$) and load-side network impedance ($Z_L$). The non-linear loads connected to the system are represented using single-phase bridge rectifiers configured with each phase. Each rectifier supplies a resistive and an inductive load on the DC side with varying values. Figure 1 shows the test system and filter configuration used in this paper.

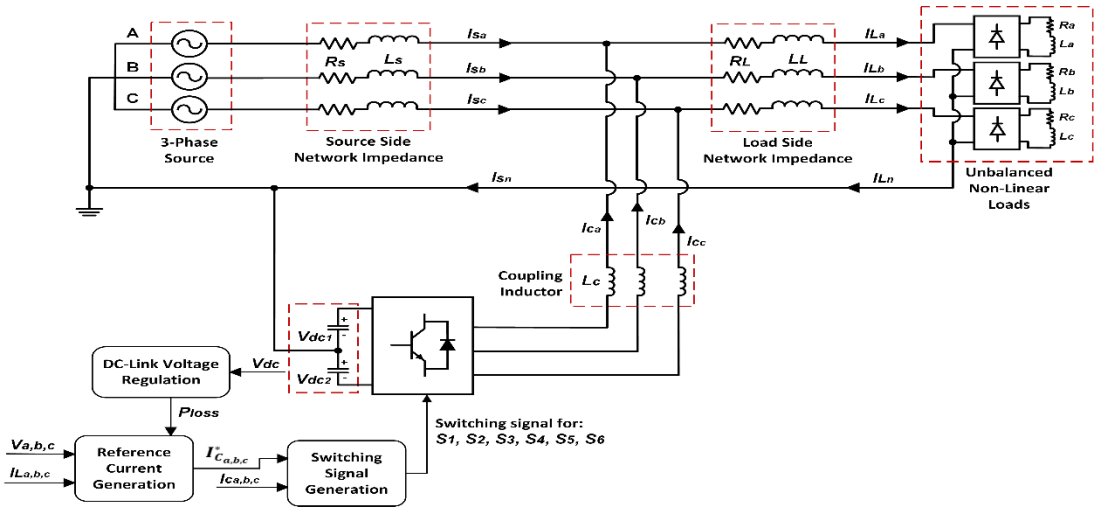


**Figure 1. Test System and Filter Configuration**

The suggested AF in this paper adopts a three-leg voltage-source inverter (VSI) with a split capacitor to compensate for current harmonic distortion and current imbalance. The AF is configured with a three-phase coupling inductor ($L_C$) that serves to filter ripple resulting from the VSI switching process.

**Control Scheme of the AF**

The suggested AF has three control units, namely DC-link voltage regulation, reference current generation, and switching signal generation. The instantaneous active and reactive power theory (IRPT) is used in this paper to generate the reference current. IRPT is known for its quick dynamic response in compensating for harmonics and balancing unbalanced load currents [18]. The IRPT scheme for generating the reference current is shown in Figure 2.

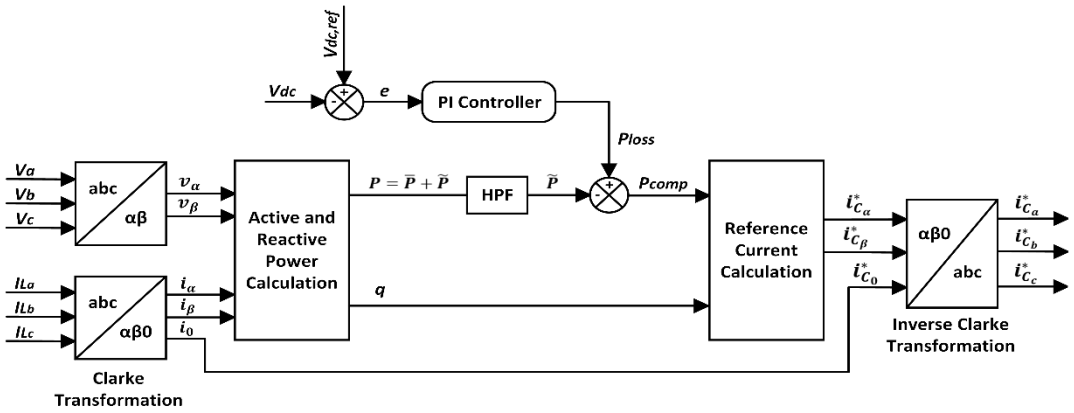


**Figure 2. IRPT Scheme for Generating the Reference Current**

In IRPT scheme, the calculations for active power ($P$) and reactive power ($q$) are based on the source voltage ($V_{a,b,c}$) and load current ($I_{La,b,c}$). Using the Clarke transformation, the source voltage and source current signals in the *abc* coordinate system are converted to voltage in the $\alpha\beta$ coordinate system ($v_{\alpha,\beta}$) and load current in $\alpha\beta 0$ coordinate system ($i_{\alpha,\beta,0}$) as in reference [19]. $i_0$ will be used as the zero-coordinate reference current ($i^*_{C_0}$), while $i_\alpha$ and $i_\beta$ with $v_\alpha$ and $v_\beta$ are used to calculate $P$ and $q$ using Equation (1).

$$\begin{bmatrix} P \\ q \end{bmatrix} = \begin{bmatrix} v_\alpha & v_\beta & 0 \\ -v_\beta & v_\alpha & 0 \end{bmatrix} \begin{bmatrix} i_\alpha \\ i_\beta \end{bmatrix} \qquad (1)$$

$P$ consists of DC component ($\bar{P}$) and AC component ($\tilde{P}$). Using a high-pass filter (HPF), $P$ is filtered to obtain $\tilde{P}$. The loss power ($P_{loss}$) is generated by the proportional-integral (PI) controller to regulate the voltage value of the DC-link capacitor at its reference value. The difference between $P_{loss}$ dan $\tilde{P}$ yields the compensation power ($P_{comp}$). From the obtained $P_{comp}$ and $q$, the $\alpha\beta$-coordinated reference current ($i^*_{C_{\alpha,\beta}}$) can be calculated using Equation (2).

$$\begin{bmatrix} i^*_{C_\alpha} \\ i^*_{C_\beta} \end{bmatrix} = \frac{P_{comp}+q_{comp}}{{v_\alpha}^2+{v_\beta}^2} \begin{bmatrix} v_\alpha \\ v_\beta \end{bmatrix} \qquad (2)$$

To be injected into the system, the reference current in $\alpha\beta 0$ coordinates ($i^*_{C_{\alpha,\beta,0}}$) is converted back to *abc* coordinates ($i^*_{C_{a,b,c}}$) using the inverse Clarke transformation as in reference [19]. Next, the reference current is used to generate the switching signals using adaptive hysteresis current control method. The bandwidth in adaptive hysteresis current control is determined based on the variation of instantaneous compensation current ($\mathrm{d}i^*_c/\mathrm{d}t$) and DC-link voltage ($V_{dc}$), while the switching frequency ($f_c$) and coupling inductor ($L_c$) are set to constant values [20], [21]. The hysteresis bandwidth (HB) for the

adaptive hysteresis current control scheme can be calculated using Equation (3).

$$\mathrm{HB} = \left\{\frac{V_{dc}}{8 f_c L}\left[1 - \frac{4L_c^2}{V_{dc}^2}\left(\frac{v_s}{L} + \frac{di_c^*}{dt}\right)^2\right]\right\} \qquad (3)$$

The calculated HB value is then compared with the reference compensation current ($i_c^*$) and the actual compensation ($i_c$) current to generate switching signals for VSI.

## Simulation Circuit Parameters

The proposed testing system in this paper was simulated using MATLAB Simulink R2020a. The simulation for this paper used a sampling time of $5\times10^{-6}$ seconds with a stop time of 2 seconds. The AF was activated at 0.5 seconds, so that all power flow and harmonic waveform analysis, as well as FFT analysis, sampled data from 1.9 seconds to 2 seconds. The parameters of the simulation circuit used in this paper are presented in Table 1.

**Table 1. Parameter Values of the Simulation Circuit**

| Parameter | Value |
|---|---|
| Source voltage | 400 V |
| System frequency | 50 Hz |
| Source side network impedance | R = $10^{-5}$ Ohm; L = $10^{-6}$ H |
| Load side network impedance | R = $10^{-6}$ Ohm; L = $10^{-4}$ H |
| Rectifier load resistance | $R_A$ = 10 Ohm; $R_B$ = 15 Ohm; $R_C$ = 5 Ohm |
| Rectifier load inductance | $L_A = L_B = L_C$ = 0.1 H |
| DC-link voltage | $V_{dc1} = V_{dc2}$ = 600 V |
| DC-link capacitor capacitance | $C_{dc1} = C_{dc1}$ = 14576 µF |
| Inverter switching frequency | 20 kHz |
| Coupling inductor inductance | 1.45 mH |
| PI controller constant | $K_P$ = 100; $K_I$ = 800 |

## Regulations for Performance Evaluation

The performance evaluation of the suggested AF in this paper is based on IEEE 519 and IEEE 1159. IEEE 519-2022 is an IEEE standard issued in 2022 for monitoring harmonic distortion in electrical systems. Similar to previous versions, IEEE 519-2022 establishes thresholds for current harmonic distortion in the form TDD percentage based on the $I_{SC}/I_L$ ratio [22]. The TDD percentage can be calculated using the $\mathrm{THD_I}$ value and the RMS value of the fundamental current ($I_{1rms}$), which can be identified using the FFT analysis feature in Simulink, as shown in Equation (4).

$$\%\mathrm{TDD} = \left(\mathrm{THD} \times \frac{I_1}{I_L}\right) \times 100\% \qquad (4)$$

The $I_{SC}$ value in this paper is 7.277 kA, which is obtained by dividing the phase-to-neutral voltage by the system impedance consisting of $Z_S$ and $Z_L$. Meanwhile, the $I_L$ value is taken from the highest current value among the three phases before compensation, namely 40.7 A. Thus, the $I_{SC}/I_L$ ratio in this paper is 178.8. The current harmonic distortion thresholds for the obtained $I_{SC}/I_L$ ratio are summarized in Table 2.

**Table 2. Current Harmonic Distortion Thresholds for $I_{SC}/I_L$ = 178.8**

| **Maximum Current Harmonic Distortion in Percent (%)** | | | | | | |
|---|---|---|---|---|---|---|
| **Odd Harmonics Order** | | | | | | |
| $I_{SC}/I_L$ | $3 \le h < 11$ | $11 \le h < 17$ | $17 \le h < 11$ | $23 \le h < 35$ | $35 \le h < 50$ | TDD |
| 178.8 | 12.0 | 5.5 | 5.0 | 2.0 | 1.0 | 15.0 |

IEEE 1159-2019 is an IEEE standard issued in 2019 for monitoring power quality in electrical systems. IEEE 1159-2019 classifies power quality disturbances into seven categories, one of which is imbalance. The typical value for current imbalance specified in IEEE 1159-2019 is 3% [7]. In addition to defining typical values, the

standard specifies a formula for calculating current imbalance in a three-phase system with four wires using Equation (5).

$$\%I_{unb} = \left|\frac{I_{neg}}{I_{pos}}\right| \times 100\% \qquad (5)$$

## RESULT

### Source Current, Load Current, and Neutral Current Profiles

Table 3 presents the simulation results, including the source current, load current, and neutral current values before and after compensation using the suggested AF.

**Table 3. Source Current, Load Current, and Neutral Current Values**

| Current | Phase | Before Compensation | After Compensation |
|---|---|---|---|
| Source current | A | 20.51 A | 23.83 A |
| | B | 13.76 A | 23.35 A |
| | C | 40.7 A | 23.44 A |
| Load current | A | 20.51 A | 20.51 A |
| | B | 13.76 A | 13.76 A |
| | C | 40.7 A | 40.7 A |
| Neutral current | N | 32.92 A | 4.32 A |

In addition to the values shown in Table 3, the source current waveforms before and after compensation were also obtained, as represented in Figure 3 and Figure 4.

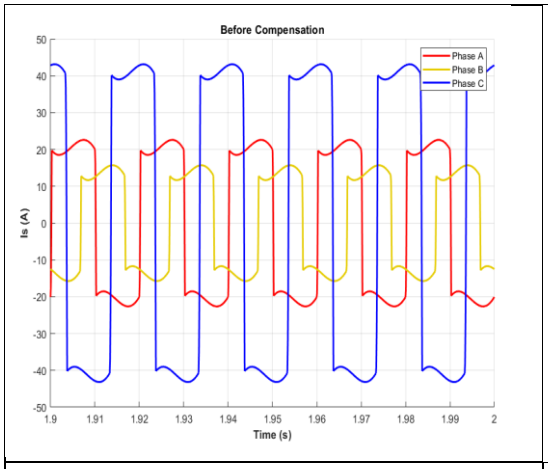


**Figure 3. Distorted Source Current**

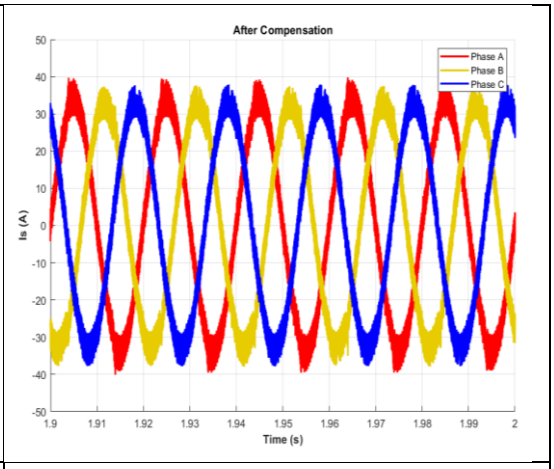


**Figure 4. Compensated Source Current**

### Current Unbalance Profiles

Table 4 presents the current imbalance profile from the simulation results, which includes the positive-sequence current ($I_{pos}$), negative-sequence current ($I_{neg}$), zero-sequence current ($I_{zero}$), the calculated current imbalance ($I_{unb}$) percentage on the source side, as well as its comparison with the typical value specified in IEEE 1159-2019.

**Table 4. Symmetrical Components Current and Current Unbalance Value**

| Condition | $I_{pos}$ | $I_{neg}$ | $I_{zero}$ | $I_{unb}$ | $I_{unb}$ Typical Value |
|---|---|---|---|---|---|
| Before Compensation | 32.35 A | 10.42 A | 10.42 A | 32.21% | 3% |
| After Compensation | 33.06 A | 0.18 A | 0.18 A | 0.54% | |

### Current Harmonic Distortion Profiles

In addition to the current and current imbalance profile, the Simulink simulation also yielded the $THD_I$ and $I_{1rms}$ values for each phase, as summarized in Table 5.

**Table 5. $THD_I$ and $I_{1rms}$ Before and After Compensation**

| Phase | Before Compensation | | After Compensation | |
|---|---|---|---|---|
| | $THD_I$ | $I_{1rms}$ | $THD_I$ | $I_{1rms}$ |
| A | 43.92% | 18.78 A | 11.24% | 23.62 A |
| B | 42.46% | 12.66 A | 11.27% | 23.21 A |
| C | 44.51% | 37.19 A | 10.92% | 23.29 A |

Based on the $THD_I$ and $I_{1rms}$ values presented in Table 5, the TDD percentage was calculated using Equation (4) and compared with the thresholds listed in Table 1. The calculated TDD percentage of each phase and its comparison with the thresholds specified in IEEE 519-2022 are presented in Figure 5.

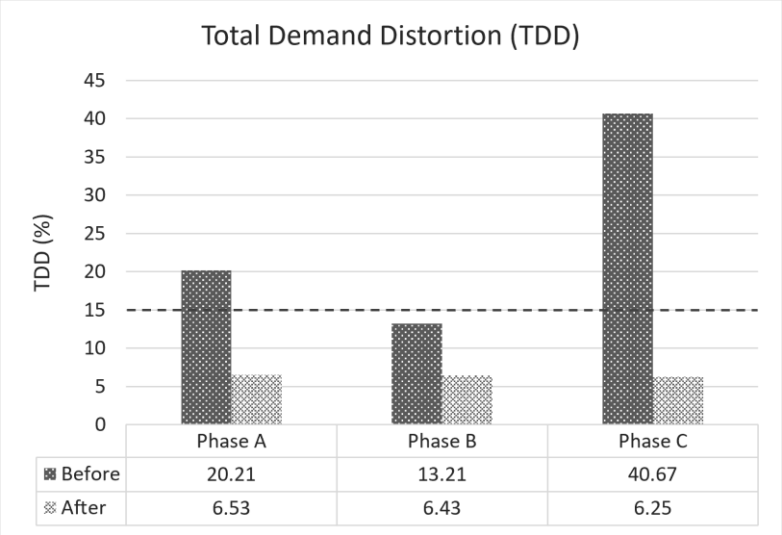


**Figure 5. TDD Percentages Before and After Compensation**

## DISCUSSION

The evaluation of the suggested AF's ability to compensate for current imbalance in this paper was conducted by examining the source current ($I_S$), load current ($I_L$), and neutral current ($I_{neutral}$) profiles presented in Table 3, Figure 3, and Figure 4, as well as by comparing the calculated $I_{unb}$ before and after compensation with the typical value shown in Table 4. Based on the $I_S$, $I_L$, and $I_{neutral}$ current profiles shown in Table 3, Figure 3, and Figure 4, it can be seen that the current unbalance on the source side has been effectively compensated using the suggested AF. The $I_S$ values of each phase were successfully balanced from 20.51 A to 23.83 A for phase A, from 13.76 to 23.35 A for phase B, and from 40.7 A to 23.44 A for phase C. This is further supported by the decrease in $I_{unb}$ following compensation, as shown in Table 4.

The $I_{unb}$ percentage of 32.21% indicates that before compensation, the system experienced a rather extreme current imbalance. The $I_{neg}$ and $I_{zero}$ values were also quite high, at 10.42 A. After compensation using the suggested AF, the $I_{unb}$ percentage was successfully reduced to 0.54%. The reduction in the $I_{unb}$ percentage was accompanied by a decrease in the negative sequence current and zero-sequence current values to 0.18 A. Consistent with the decrease in $I_{zero}$, the $I_{neutral}$ value also decreased from an initial 32.92 A to 4.32 A. This is because in a three-phase system with four wires, $I_{zero}$ add up in the neutral wire.

In this paper, the evaluation examines not only the ability to compensate for current imbalance, but also the AF's ability to compensate for current harmonic distortion. The evaluation of the proposed AF's ability to compensate for current harmonic distortion in this paper was conducted by

comparing the TDD percentages before and after compensation. It can be seen from Figure 5 that the suggested AF successfully reduced the TDD in phase A from 20.21% to 6.53%, in phase B from 13.21% to 6.43%, and in phase C from 40.67% to 6.25%. The TDD percentage after compensation across all phases successfully met the limit value of 15% specified in Table 2. Based on the overall results obtained, it indicates that the suggested AF in this paper demonstrates capable performance in compensating for both current unbalance and current harmonic distortion occurring at the same time in a three-phase system with four wires.

## CONCLUSION

In this paper, the compensation performance for current harmonic distortion and current unbalance of an AF with three phases and four wires was evaluated in accordance with IEEE 519-2022 and IEEE 1159-2019. Through a series of testing processes using MATLAB Simulink, results were obtained showing that the suggested AF is capable of compensating for current unbalance and current harmonic distortion at the same time. This achievement is evident in the reduction of the current unbalance percentage and TDD to meet the threshold value of 3% set in IEEE 1159-2019 and 15% set in IEEE 519-2022. The determination of the IEEE 519-2022 standard used in this paper is based on the calculated $I_{SC}/I_L$ ratio. The reduction in the zero-sequence value, resulting from the reduction in, also leads to a decrease in the neutral current value, thereby minimizing the potential negative impact of high neutral current.

### *Declaration by Authors*

**Acknowledgement:** The authors thanks to Electrical Department and Faculty of Engineering, Diponegoro University for supporting the work through fundamental research grant 2026

**Source of Funding:** None

**Conflict of Interest:** No conflicts of interest declared.

## REFERENCES

1. A. Baggini, Handbook of Power Quality. Wiley, 2008. doi: 10.1002/9780470754245.
2. N. Keerthi, A. Pandian, and R. Dhanasekaran, “A Comprehensive Study on Shunt Active Power Filters for Grid – Tied wind systems,” IOP Conf. Ser. Mater. Sci. Eng., vol. 993, no. 1, p. 012085, Dec. 2020, doi: 10.1088/1757-899X/993/1/012085.
3. S. Chattopadhyay, M. Mitra, and S. Sengupta, Electric Power Quality. in Power Systems. Dordrecht: Springer Netherlands, 2011. doi: 10.1007/978-94-007-0635-4.
4. E. F. Fuchs and M. A. S. Masoum, Power Quality in Power Systems, Electrical Machines, and Power-Electronic Drives. Elsevier, 2023. doi: 10.1016/C2018-0-02457-3.
5. S. R. Das et al., “A comprehensive survey on different control strategies and applications of active power filters for power quality improvement,” Energies, vol. 14, no. 15, 2021, doi: 10.3390/en14154589.
6. A. Lucas, F. Bonavitacola, E. Kotsakis, and G. Fulli, “Grid harmonic impact of multiple electric vehicle fast charging,” Electr. Power Syst. Res., vol. 127, pp. 13–21, Oct. 2015, doi: 10.1016/j.epsr.2015.05.012.
7. T. and D. Committee of IEEE Power and Energy Society, “IEEE Recommended Practice for Monitoring Electric Power Quality.” IEEE, Piscataway, NJ, USA, p. 94, Jun. 13, 2019. doi: 10.1109/IEEESTD.2019.8796486.
8. B. Misra, P. Tripathy, R. Mohanty, S. R. Sahoo, and B. Nayak, “Performance Analysis of an Adaptive Hysteresis Band Current Controller based Active Power Filter,” in 2022 2nd International Conference on Advances in Electrical, Computing, Communication and Sustainable Technologies, ICAECT 2022, IEEE, Apr. 2022, pp. 1–5. doi: 10.1109/ICAECT54875.2022.9807992.
9. P. Karuppanan, S. R. Prusty, and K. Mahapatra, “Adaptive-hysteresis current controller based active power filter for power quality enhancement,” in International Conference on Sustainable Energy and Intelligent Systems (SEISCON 2011), IET, 2011, pp. 1–6. doi: 10.1049/cp.2011.0325.
10. V. Singh, S. J. Iqbal, S. Gupta, and A. Yadav, “Performance Evaluation of A Shunt Active Power Filter For Current Harmonic Elimination,” in 2021 IEEE Region 10

Symposium (TENSYMP), IEEE, Aug. 2021, pp. 1–6. doi: 10.1109/TENSYMP52854.2021.9550846.
11. A. Andang, R. S. Hartati, I. B. Gede Manuaba, and I. N. Satya Kumara, "Three-phase four-wire shunt hybrid active power filter model with model predictive control in imbalance distribution networks," Int. J. Electr. Comput. Eng., vol. 12, no. 6, p. 5923, Dec. 2022, doi: 10.11591/ijece. v12i6.pp5923-5937.
12. A. A. Eid, A. M. A. Soliman, and M. A. Mehanna, "Optimize Gain Values of PI-Controller for Active Power Filter Using Mayfly Algorithm," Int. J. Renew. Energy Res., vol. 12, no. V12i4, pp. 1727–1735, 2022, doi: 10.20508/ijrer. v12i4. 13413.g8597.
13. Y. Bekakra, L. Zellouma, and O. Malik, "Improved predictive direct power control of shunt active power filter using GWO and ALO – Simulation and experimental study," Ain Shams Eng. J., vol. 12, no. 4, pp. 3859–3877, Dec. 2021, doi: 10.1016/j.asej.2021.04.028.
14. A. Mostefa, K. Belalia, T. Lantri, H. M. Boulouiha, and A. Allali, "A four-line active shunt filter to enhance the power quality in a microgrid," Int. J. Renew. Energy Dev., vol. 12, no. 3, pp. 488–498, May 2023, doi: 10.14710/ijred.2023.50270.
15. T. Bo, L. Haidong, Y. Xiwen, and Z. Ruijin, "Configuration and dimension optimization of active power Filter in distribution networks using a Multi-Strategy improved algorithm," Int. J. Electr. Power Energy Syst., vol. 168, no. March 2024, p. 110677, Jul. 2025, doi: 10.1016/j.ijepes.2025.110677.
16. R. Vlasenko, O. Bialobrzheskyi, and A. Gladyr, "Four-Wire Three-Phase Active Power Filter With Fuzzy Controller For Compensation Of Distortion of Currents Unbalance in the Conditions of Fluctuated Load," in 2019 IEEE International Conference on Modern Electrical and Energy Systems (MEES), IEEE, Sep. 2019, pp. 222–225. doi: 10.1109/MEES.2019.8896448.
17. L. F. A. Maciel, J. L. M. Morales, D. C. Gaona, and J. G. M. Pimentel, "A Study of a Three-Phase Four-Wire Shunt Active Power Filter for Harmonics Mitigation," in 2018 IEEE International Autumn Meeting on Power, Electronics and Computing (ROPEC), IEEE, Nov. 2018, pp. 1–6. doi: 10.1109/ROPEC.2018.8661416.
18. D. M. Soomro, S. K. Alswed, M. N. Abdullah, N. H. M. Radzi, and M. H. Baloch, "Optimal design of a single-phase APF based on PQ theory," Int. J. Power Electron. Drive Syst., vol. 11, no. 3, p. 1360, Sep. 2020, doi: 10.11591/ijpeds. v11.i3. pp1360-1367.
19. H. Akagi, E. H. Watanabe, and M. Aredes, Instantaneous Power Theory and Applications to Power Conditioning. Wiley, 2017. doi: 10.1002/9781119307181.
20. S. Handoko and B. Winardi, "Comparison of Conventional and Adaptive Hysteresis Current Control Methods for Power Quality Improvement using Active Filters," Adv. Sustain. Sci. Eng. Technol., vol. 7, no. 4, p. 0250403, Aug. 2025, doi: 10.26877/asset. v7i4.1981.
21. M. Kale and E. Ozdemir, "An adaptive hysteresis band current controller for shunt active power filter," Electr. Power Syst. Res., vol. 73, no. 2, pp. 113–119, Feb. 2005, doi: 10.1016/j.epsr.2004.06.006.
22. T. and D. Committee of IEEE Power and Energy Society, "IEEE Standard for Harmonic Control in Electric Power Systems." IEEE, Piscataway, NJ, USA, p. 31, May 13, 2022. doi: 10.1109/IEEESTD.2022.9848440.

How to cite this article: Tazkiya Muthmainnah Sukmawati, Susatyo Handoko, Mochammad Facta, Trias Andromeda, Karnoto. Active filter solution for three-phase system four wires under unbalanced and harmonics condition. *International Journal of Research and Review*. 2026; 13(6): 190-197. DOI: *https://doi.org/10.52403/ijrr.20260619*

******